Dimensionality Effects on the Optical Properties of $(PO_2)_4(WO_3)_{2m}$ (m = 2, 4, 6, 7)

Z.-T. Zhu†

Department of Chemistry, State University of New York at Binghamton, Binghamton, New York 13902

J. L. Musfeldt*

Department of Chemistry, University of Tennessee, Knoxville, Tennessee 37996

H.-J. Koo and M.-H. Whangbo

Department of Chemistry, North Carolina State University, Raleigh, North Carolina 27695

Z. S. Teweldemedhin and M. Greenblatt

Department of Chemistry, Rutgers, the State University of New Jersey, Piscataway, New Jersey 08855

Received December 5, 2001. Revised Manuscript Received March 19, 2002

We report the 300 K polarized reflectance spectra and calculated electronic band structures of a series monophosphate tungsten bronzes, $(PO_2)_4(WO_3)_{2m}$ (m = 2, 4, 6, 7). These materials have several layers of corner-sharing WO_6 octahedra separated by one PO_4 layer, leading to an octahedral layer thickness that is "tunable" with m. In the optical regime, the spectra of the m = 2, 4, 6, and 7 materials display an anisotropic electronic excitation, originating from the W intra-t_{2g} d → d transition. The intensity and frequency of the intra-t_{2g} d → d excitation vary with the octahedral layer thickness. Several vibrational modes along the interlayer direction of the m = 4, 6, and 7 compounds change with m as well. These results are consistent with the lattice becoming softer with increasing m. The low-frequency electrodynamics of the monophosphate tungsten bronzes shows a gap or pseudogap feature in the infrared region, demonstrating a ubiquitous bound-carrier response in these tungsten bronzes.

I. Introduction

Charge density waves (CDWs) in two-dimensional (2D) materials such as monophosphate tungsten bronzes (MPTBs) are of recent interest.[1−3] This is because less is known about density wave instabilities in layered materials than in the prototypical one-dimensional (1D) compounds.[4−14] MPTBs are a series of quasi-two-dimensional (Q2D) materials with the general chemical formula $(PO_2)_4(WO_3)_{2m}$, where m = 2−14. The structures of these materials contain perovskite-type corner-sharing WO_6 octahedral layers; these layers are connected by PO_4 tetrahedra, as shown in Figure 1 for the m = 2, 4, 6, and 7 compounds. The m = 2, 4, and 6 compounds are orthorhombic, whereas the m = 7 material is pseudo-orthorhombic (monoclinic with β = 90.19°).[15] For m = 4−14, the interlayer direction is defined as the c axis, and the octahedral layers are in the ab plane; for m = 2, the chains of corner-sharing WO_6 octahedra are along the c axis, and the interlayer direction is the b axis. The WO_6 layer thickness increases with increasing m. The WO_6 octahedra are distorted in these materials, and the distortion becomes smaller with increasing m as well. This is because the W atoms have slightly different local environments in each compound.[16] For instance, in the m = 4 material, the W atoms at the center of the WO_6 layer are

* Corresponding author. E-mail: musfeldt@utk.edu.
† Current address: Department of Materials Science and Engineering, Cornell University, Ithaca, New York 14853.

(1) Greenblatt, M. *Acc. Chem. Res.* **1996**, *29*, 219.
(2) Gabovich, A. M.; Voitenko, A. I. *Low Temp. Phys.* **2000**, *26*, 305.
(3) Klemm, R. A. *Physica C* **2000**, *341*, 839.
(4) Karecki, D. R.; Clayman, B. P. *Phys. Rev. B* **1979**, *19*, 6367.
(5) Etemad, S. *Phys. Rev. B* **1981**, *24*, 4959.
(6) Travaglini, G.; Wachter, P. *Phys. Rev. B* **1984**, *30*, 1971.
(7) Degiorgi, L.; Wachter, P.; Greenblatt, M.; McCarroll, W. H.; Ramanujachary, K. V.; Marcus, J.; Schlenker, C. *Phys. Rev. B* **1988**, *38*, 5821.
(8) Jandl, S.; Banville, M.; Pépin, C.; Marcus, J.; Schlenker, C. *Phys. Rev. B* **1989**, *40*, 12487.
(9) Degiorgi, L.; Grüner, *Synth. Met.* **1993**, *56*, 2688.
(10) Gorshunov, B. P.; Volkov, A. A.; Kozlov, G. V.; Degiorgi, L.; Blank, A.; Csiba, T.; Dressel, M.; Kim, Y.; Schwartz, A.; Grüner, G. *Phys. Rev. Lett.* **1994**, *73*, 308.
(11) Kanner, G. S.; Gammel, J. T.; Love, S. P.; Johnson, S. R.; Scott, B.; Swanson, B. I. *Phys. Rev. B* **1994**, *50*, 18682.
(12) Schwartz, A.; Dressel, M.; Alavi, B.; Blank, A.; Dubois, S.; Grüner, G.; Gorshunov, B. P.; Volkov, A. A.; Kozlov, G. V.; Thieme, S.; Degiorgi, L. *Phys. Rev. B* **1995**, *52*, 5643.
(13) Bardeau, J.-F.; Bulou, A.; Swanson, B. I.; Hennion, B. *Phys. Rev. B* **1998**, *58*, 2614.
(14) Brozik, J. A.; Scott, B. L.; Swanson, B. I. *J. Phys. Chem. B* **1999**, *103*, 10566.
(15) Roussel, P.; Labbé, P.; Groult, D. *Acta Crystallogr.* **2000**, *56*, 377.
(16) Roussel, P.; Labbé, P.; Groult, D.; Domengès, B.; Leligny, H.; Grebille, D. *J. Solid State Chem.* **1996**, *122*, 281.

10.1021/cm011675j CCC: $22.00
Published on Web 05/04/2002

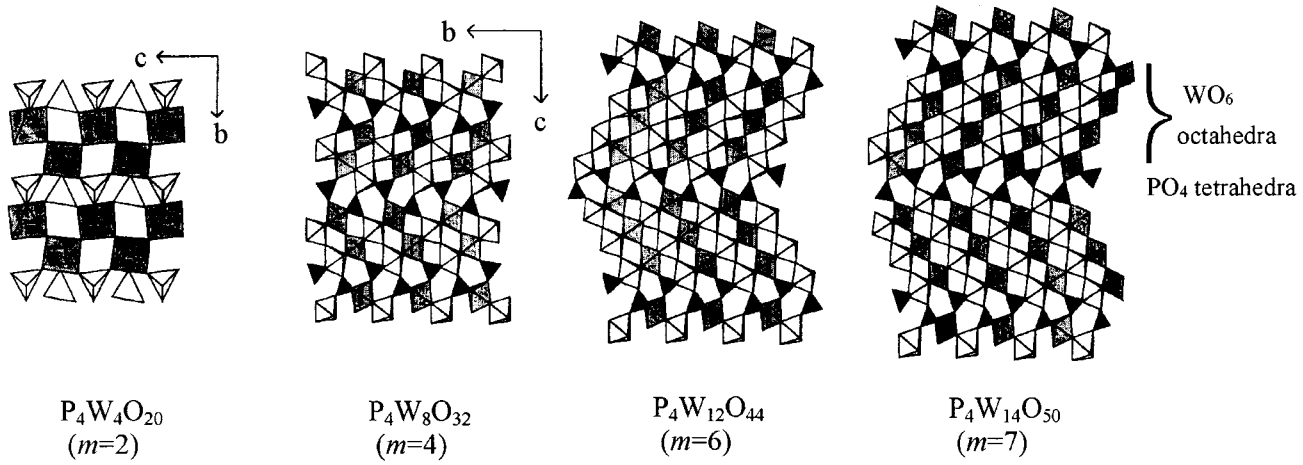

Figure 1. Crystal structures of $(PO_2)_4(WO_3)_{2m}$ compounds for various values of m. All compounds are essentially orthorhombic, making our comparisons within the same structural type.

connected to one PO_4 tetrahedron, whereas the W atoms at the edge are connected to two PO_4 tetrahedra. In the $m = 7$ compound, the W atoms are in four different environments. These subtle structural differences influence the electronic and vibrational patterns of the MPTBs.[17]

The electronic structures of the $m = 2$, 4, and 6 MPTBs have been explored in the past by the extended Hückel tight-binding (EHTB) method.[17−20] Because of their layered nature, MPTBs have Q2D electronic structures, although their Fermi surfaces exhibit "hidden" 1D topology.[21,22] The conduction bands, i.e., the bottom three t_{2g}-block bands, of these tungsten materials are similar because of the related crystal structures and W d-orbital interaction patterns. In all of the MPTBs, each WO_6 slab has two conduction electrons per unit cell. Therefore, with increasing m, the average d-electron density on W decreases, and the average oxidation state of W increases. In addition, in each MPTB, the oxidation states of the inequivalent W atoms are different because of the aforementioned different structural environments. MPTBs also provide a system with tunable interlayer interactions. The interactions between conduction electrons in different layers become weaker with increasing layer thickness (m), leading to dimensionality changes with m. Therefore, the MPTB materials provide a model system with variable layer thicknesses, octahedral distortion, nonuniform W oxidation states, tunable dimensionality, and variable interlayer interactions. These m-dependent parameters are closely related to both the physical properties of MPTBs and their CDW transitions, as summarized below.

The Q2D physical properties and low-temperature CDW instabilities in the $m = 4$, 6, and 7 tungsten bronzes have been characterized by transport, X-ray diffraction, thermopower, and infrared spectroscopy experiments.[23−33] In all of the MPTBs, the *ab*-plane conductivity is at least 1 order of magnitude larger than the conductivity along the interlayer direction. Note that the $m = 7$ sample has a superconducting transition at ~0.3 K after two successive CDW transitions[34] and is thus a member of the interesting class of "density wave superconductors".[2,3] The temperature dependence of the vibrational properties of the $m = 6$ compound suggests that the CDW transition below 120 K is associated with the central portion of the WO_6 layer,[32] in agreement with structural results on the $m = 4$ compound.[31] For the $m = 2$ sample, the temperature dependence of the resistivity along the highest-conducting c direction shows semiconducting behavior down to ~50 K.[24] The $m = 2$ compound also displays antiferromagnetic ordering at low temperature.[24]

In this work, we report the 300 K optical response of the $m = 2$, 4, 6, and 7 MPTB compounds along the three principal crystallographic directions over a wide frequency range. Our goal is to probe the effect of dimensionality on the electronic excitations, the low-frequency optical conductivity, the interlayer response, and phonons. To interpret our experimental results, we calculated new electronic band structures of the $m = 2$, 4, 6, and 7 MPTBs using the EHTB method.[35,36] Because the $m = 2$, 4, 6, and 7 MPTBs are similar in structure,

(17) Canadell, E.; Whangbo, M.-H.; Rachidi, I. E. *Inorg. Chem.* **1991**, *29*, 3871.
(18) Canadell, E.; Whangbo, M.-H. *J. Solid State Chem.* **1990**, *86*, 131.
(19) Canadell, E.; Whangbo, M.-H. *Phys. Rev. B* **1991**, *43*, 1894.
(20) Canadell, E.; Whangbo, M.-H. *Chem. Rev.* **1991**, *91*, 965.
(21) Whangbo, M.-H.; Canadell, E.; Foury, P.; Pouget, J.-P. *Science* **1991**, *252*, 96.
(22) Sandre, E.; Foury-Leylekian, P.; Ravy, S.; Pouget, J.-P. *Phys. Rev. Lett.* **2001**, *86*, 5100.
(23) Wang, E.; Greenblatt, M.; Rachidi, I. E.-I.; Canadell, E.; Whangbo, M.-H.; Vadlamannati, S. *Phys. Rev. B* **1989**, *39*, 12969.
(24) Teweldemedhin, Z. S.; Ramanujachary, K. V.; Greenblatt, M. *J. Solid State Chem.* **1991**, *95*, 21.
(25) Teweldemedhin, Z. S.; Ramanujachary, K. V.; Greenblatt, M. *Phys. Rev. B* **1992**, *46*, 7897.
(26) Foury, P.; Pouget, J. P. *Int. J. Mod. Phys. B* **1993**, *7*, 3973.
(27) Ottolenghi, A.; Foury, P.; Pouget, J. P.; Teweldemedhin, Z. S.; Greenblatt, M.; Groult, D.; Marcus, J.; Schlenker, C. *Synth. Met.* **1995**, *70*, 1301.
(28) Foury, P.; Roussel, P.; Groult, D.; Pouget, J. P. *Synth. Met.* **1999**, *103*, 2624.
(29) Dumas, J.; Hess, C.; Schlenker, C.; Bonfait, G.; Marin, E. G.; Groult, D.; Marcus, J. *Eur. Phys. J. B* **2000**, *14*, 73.
(30) Roussel, P.; Labbé, P.; Leligny, H.; Groult, D.; Foury-Leylekian, P.; Pouget, J. P. *Phys. Rev. B* **2000**, *62*, 176.
(31) Ludecke, J.; Jobst, A.; van Smaalen, S. *Europhys. Lett.* **2000**, *49*, 357.
(32) Zhu, Z.-T.; Musfeldt, J. L.; Teweldemedhin, Z. S.; Greenblatt, M. *Chem. Mater.* **2001**, *13*, 2940.
(33) Zhu, Z.-T.; Musfeldt, J. L.; Teweldemedhin, Z. S.; Greenblatt, M. *Phys. Rev. B*, in press.
(34) Hess, C.; Schlenker, C.; Bonfait, G.; Ohm, T.; Paulsen, C.; Dumas, D.; Teweldemedhin, Z.; Greenblatt, M.; Marcus, J.; Almeida, M. *Solid State Commun.* **1997**, *104*, 663.
(35) Whangbo, M.-H.; Hoffmann, R. *J. Am. Chem. Soc.* **1978**, *100*, 6093.

Table 1. Exponents ζ_i and Valence-Shell Ionization Potentials H_{ii} of the Slater-type Orbitals χ_i Used for the Extended Hückel Tight-Binding Calculation[a]

atom	χ_i	H_{ii} (eV)	ζ_1	c_1[b]	ζ_2	c_2[b]
W	5s	−8.3	2.281	1.0		
W	5p	−5.2	1.690	1.0		
W	4d	−10.4	4.151	0.5752	2.176	0.5799
P	3s	−18.6	2.367	0.5846	1.499	0.5288
P	3p	−14.0	2.065	0.4908	1.227	0.5940
O	2s	−32.3	2.688	0.7076	1.675	0.3745
O	2p	−14.8	3.694	0.3322	1.659	0.7448

[a] H_{ii}'s are the diagonal matrix elements $\langle\chi_i|H^{\text{eff}}|\chi_i\rangle$, where H^{eff} is the effective Hamiltonian. In our calculations of the off-diagonal matrix elements $H_{ij} = \langle\chi_i|H^{\text{eff}}|\chi_j\rangle$, the weighted formula was used (see Ammeter, J.; Bürgi, H.-B.; Thibeault, J.; Hoffmann, R. *J. Am. Chem. Soc.* **1978**, *100*, 3686). [b] Coefficients used in the double-ζ Slater-type orbital expansion.

this comparative investigation provides important insight into their optical properties, which we discuss in terms of dimensionality and lattice changes.

II. Methods

Single crystals of the $m = 2$, 4, 6, and 7 MPTB compounds were prepared by standard vapor-transport techniques. The crystals of the $m = 4$, 6, and 7 samples are platelike, with the large face defined by the conducting *ab* plane. The crystal of the $m = 2$ sample is needlelike. The phase of each sample was checked by X-ray diffraction; no oxygen nonstoichiometry was found.

Several spectrometers were used to cover our investigated frequency range as appropriate. A Bruker 113v Fourier transform infrared (FTIR) spectrometer equipped with a He-cooled bolometer and DTGS detectors and a modified Perkin-Elmer λ-900 spectrometer were employed for the frequency range from 50 to 45 000 cm^{-1}. The far-infrared spectrum for the $m = 6$ compound is unfortunately not available because of the small crystal size and is the exception. For the small $m = 6$ crystal and the crystal edges of the $m = 4$ and 7 materials, a Bruker Equinox 55 FTIR spectrometer coupled to a Bruker IR Scope II instrument was used with several detectors and objectives to cover the frequency range 600−16 000 cm^{-1}. The microscope has the advantage of a very small spot size. The *a*-axis spectrum of the $m = 2$ sample is nearly identical to the *b*-axis response from 600 to 16 000 cm^{-1}, therefore, we will refer to the polarizations of the spectra as $\|c$ (along the needle direction) and $\perp c$. The principal polarization axes were determined to be those displaying the greatest anisotropy at 300 K. A Kramers−Kronig analysis of the reflectance spectra was used to obtain the optical constants of the $m = 2$, 4, 6, and 7 materials. Here, only the spectra between 50 and 16 000 cm^{-1} are reported.

The electronic band structures of the $m = 2$, 4, 6, and 7 compounds were calculated using EHTB methods. Compared to previous work, an improved basis set was used.[20] Our EHTB calculations were carried out using the double-ζ Slater-type orbitals (DZ-STOs) not only for the W 4d orbitals but also for the O 2s/2p and P 3s/3p orbitals. This approach provides a much better description of the electronic structures of transition metal oxides than does the conventional approach in which transition metal elements are represented by DZ-STOs, but main group elements are represented by single-ζ Slater-type orbitals.[17−20] The atomic orbital parameters used in our EHTB calculations are summarized in Table 1. Additionally, this work presents the band structure of the $m = 7$ material for the first time, as well as the electronic structure along the interlayer direction for all of the compounds of interest here. Band structures along all three crystal axes are used to assign the spectral features and understand the *m*-dependent trends in these MPTB compounds.

(36) Our calculations were carried out using the CAESAR program package (Ren, J.; Liang, W.; Whangbo, M.-H. *Crystal and Electronic Structure Analysis Using CAESAR*; PrimeColor Software: Cary, NC, 1998; http://www.PrimeC.com/).

III. Results and Discussion

A. 300 K Reflectance and Optical Conductivity Spectra of $(PO_2)_4(WO_3)_{2m}$. Figure 2 shows the 300 K reflectance spectra along the three principal polarization axes of the four MPTB compounds studied here. For the $m = 2$ material, the reflectance in the *c* (chain) direction is significantly higher than that in the $\perp c$ direction, consistent with the 1D character of this compound. In the infrared regime, several vibrational modes are observed along both polarizations. At high frequencies, a weak electronic excitation is observed along both directions. Note that the reflectance spectra are nearly isotropic along the *a* and *b* axes; this response is labeled as $\perp c$ in the upper left-hand panel of Figure 2. The optical spectra of the $m = 4$, 6, and 7 materials are quite different from that of the $m = 2$ compound. Below 2000 cm^{-1}, the reflectance is high and nearly isotropic in the conducting *ab* plane, whereas the *c*-axis response is dominated by strong vibrational features and a low background reflectance. For the $m = 4$ compound, a clear dip is observed in the far-infrared *ab*-plane reflectance spectra near 500 cm^{-1}. Anisotropic electronic excitations are also observed along the three principal-axis directions of the $m = 4$, 6, and 7 materials. The intensity and position of these excitations vary with *m*, as discussed in the next section.

Figure 3 displays the optical conductivities of the $m = 2$, 4, 6, and 7 compounds in the 50−16 000 cm^{-1} frequency range. For the $m = 2$ sample, no free-carrier (Drude) response is observed down to 50 cm^{-1}; instead, a broad structure centered at ∼2000 cm^{-1} is present along the chain direction (*c*), characteristic of a weakly metallic, low-dimensional material. The *ab*-plane optical conductivity of the $m = 4$ material is dominated by a strong infrared absorption, characteristic of bound-carrier localization and gap, whereas the low-frequency spectra of the $m = 6$ and 7 materials show an apparent metallic (free-carrier) response, with additional oscillator strength in the middle infrared range. Along the interlayer direction, the optical conductivity is low, with several strong vibrational features in the infrared regime. At higher energy, anisotropic electronic excitations are observed along all distinct polarization directions in the optical conductivity spectra of the $m = 2$, 4, 6, and 7 compounds. Thus, the electrodynamic response in the optical regime is not isotropic in the conducting *ab* plane, as might be anticipated for a 2D layered material, highlighting the underlying 1D character of the electronic structure in the MPTB family. In the sections below, we discuss the *m* dependence of the high-frequency electronic excitations, the unusual low-frequency electrodynamics, and the *c*-axis phonons.

B. Electronic Structure of $(PO_2)_4(WO_3)_{2m}$ as a Function of *m*. *1. Excitation Assignments.* We assigned the anisotropic electronic excitations observed in Figure 3 according to the band structures of the $m = 2$, 4, 6, and 7 MPTBs obtained from our current EHTB calculations. Figure 4 shows band dispersion relations along the three crystallographic directions for all four compounds. Figure 5 shows the corresponding density of states (DOS) plots. Here, we concentrate on the energy

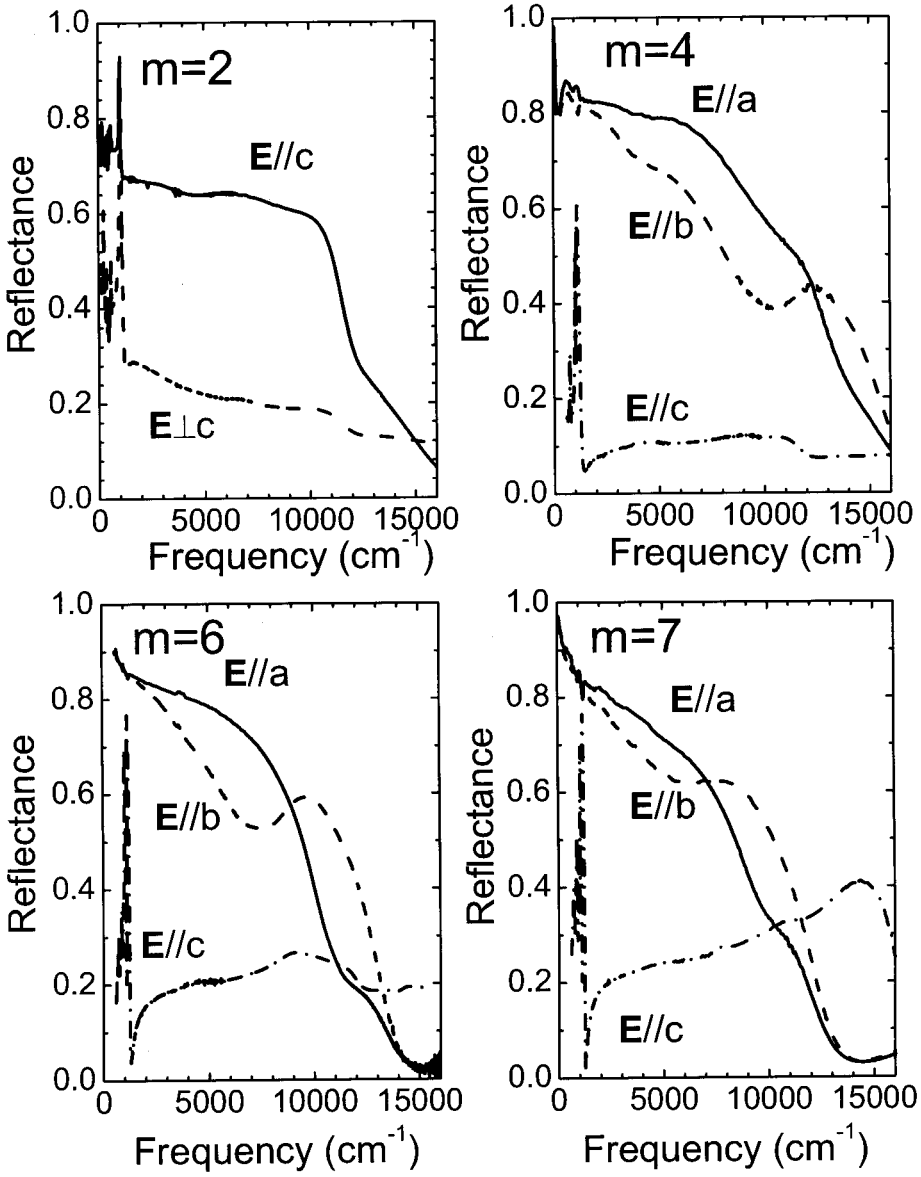

Figure 2. Polarized reflectance spectra of the $m = 2$, 4, 6, and 7 MPTB compounds at 300 K.

region of the O p bands and the W t_{2g} bands. The W e_g bands are not shown because their bottom lies more than 5 eV above the top of the t_{2g} bands for all MPTBs. For the $m = 2$ material, only one band along the *c* direction is dispersive (Figure 4a). For the $m = 4$, 6, and 7 materials, there are two types of dispersive t_{2g} bands; the first type is dispersive only along the *a* direction, and the other type is dispersive along both the *a* and *b* directions of the WO_6 layer (Figure 4). Therefore, the t_{2g} bands of the $m = 2$ MPTB have 1D character, whereas those of the $m = 4$, 6, and 7 MPTBs have both 1D and 2D character. The bottom of the t_{2g} bands lies more than 3 eV above the top of the p-block bands for the MPTBs. The Fermi level occurs near the bottom of the t_{2g} block, and the width of the t_{2g} bands is ~2 eV for $m = 2$ and ~3 eV for $m = 4$, 6, and 7.

Judging from these calculations, the optical transitions presented in Figures 2 and 3 are assigned as intra-t_{2g} d → d excitations, i.e., transitions from the filled t_{2g} bands to the empty t_{2g} bands. This assignment is consistent with those of of η- and γ-Mo_4O_{11}, which have crystal structures similar to those of MPTBs.[37] A comparison of Figures 2 and 4 shows that a high reflectance along a given crystallographic direction correlates with dispersive t_{2g} bands along that direction. Figure 4 shows that the t_{2g} bands are flat along the interlayer direction for all of the $m = 2$, 4, 6, and 7 MPTBs, in agreement with the semiconducting character of the experimental spectra. The very intense O p → W d charge-transfer excitation, observed at ~35 000 cm^{-1} (not shown),[33] is also in good agreement with these band structure calculations.

2. m Dependence of the Intra-t_{2g} Excitations. The resonance frequency of the intra-t_{2g} d → d electronic excitation in the MPTBs depends on the layer thickness and polarization direction, as shown in Figure 6. The electronic intra-t_{2g} transition is nearly isotropic for the $m = 2$ and 4 crystals, whereas the anisotropy becomes quite pronounced in the $m = 6$ and 7 materials. This is because the *b*-polarized intra-t_{2g} transition red shifts with increasing *m*. The *a*-polarized excitation is only

(37) Zhu, Z.; Chowdhary, S.; Long, V. C.; Musfeldt, J. L.; Koo, H.-J.; Whangbo, M.-H.; Wei, X.; Negishi, H.; Inoue, M.; Sarrao, J.; Fisk, Z. *Phys. Rev. B* **2000**, *61*, 10057.

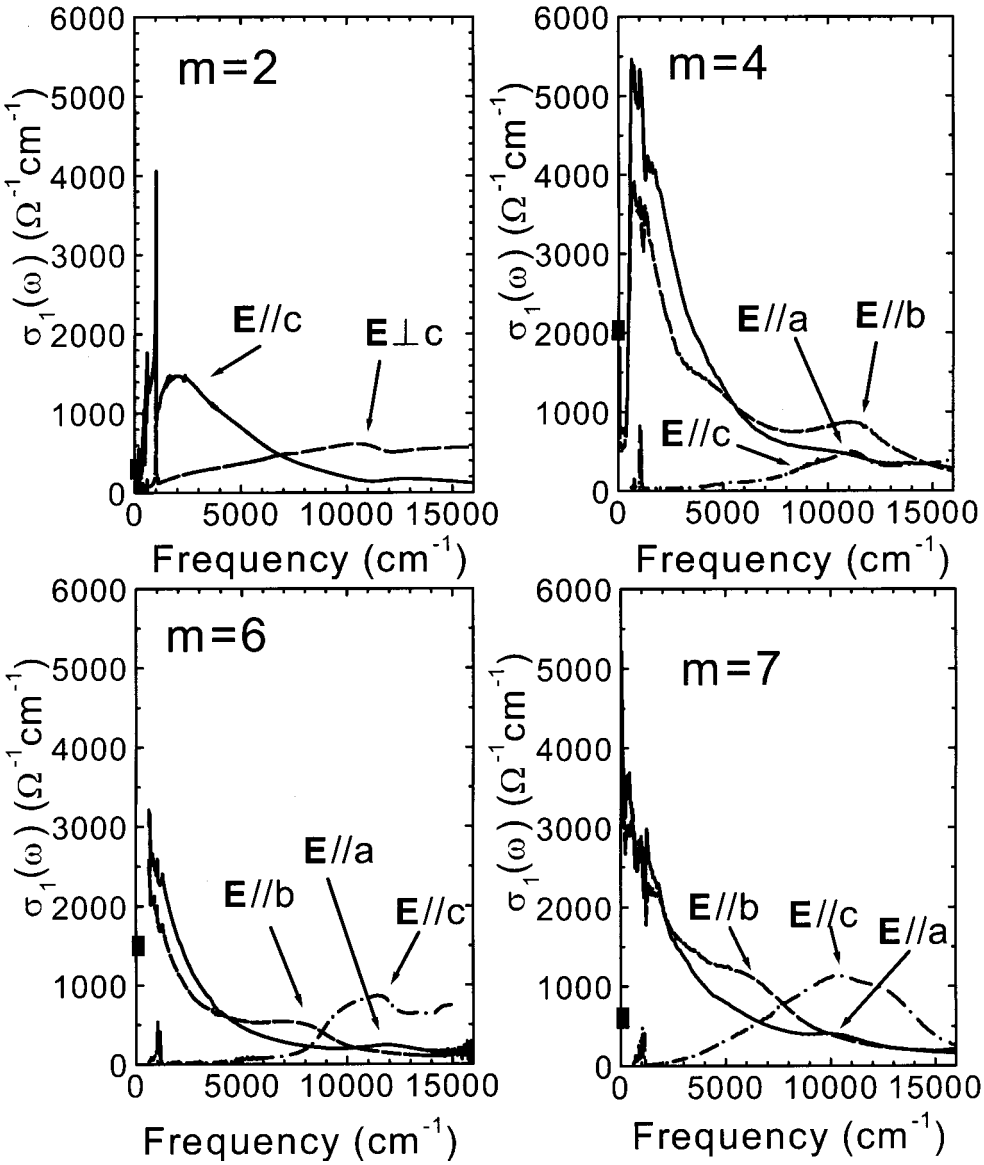

Figure 3. Optical conductivities of the $m = 2$, 4, 6, and 7 MPTB compounds at 300 K. All data are shown on the same conductivity scale to facilitate comparison. The dc conductivity of each material[23−25,29] is indicated by a solid square at zero frequency.

slightly affected by m. The interlayer (c) response is nearly m-independent as well.

At present, we are unable to conclusively explain these trends in terms of the calculated band structures. Nevertheless, it is interesting to note how the band dispersion relations of the $m = 4$, 6, and 7 MPTBs differ along the three crystallographic directions. Figure 4 shows that the t_{2g} bands are all flat along the interlayer c direction, and are all dispersive along the a direction. However, along the b direction, the electronic structure consists of both flat and dispersive bands. It is possible that the dimensional sensitivity of the b-polarized excitation (Figure 6) is related to the lattice relaxation, which increases with m.

Although the center position does not depend on the layer thickness, the general character of the intra-t_{2g} electronic excitation along the interlayer direction is highly m-dependent. As shown in Figure 3, this excitation becomes stronger and broader with increasing m. For the $m = 7$ compound, the feature is ∼7000 cm^{-1} wide and possibly composed of several overlapping excitations. This trend might be related to the increased octahedral layer thickness and the consequent different oxidation states of W across the same octahedral layer.

C. Dimensionality Effects on the Infrared Electrodynamics. *1. ab-Plane Response.* In this section, we compare the low-frequency electrodynamics of the $m =$ 2, 4, and 7 MPTBs (Figure 7). We show that the characteristic charge localization in the $m = 2$ and 4 materials is also present (but hidden) in the b-polarized spectrum of the $m = 7$ density wave superconductor. Interestingly, this bound-carrier absorption is not predicted by band structure calculations.

For the $m = 2$ material, the frequency-dependent conductivity along the c direction is characteristic of a weak metal with a broad absorption centered near ∼2000 cm^{-1}, whereas a semiconducting response is observed along the $\perp c$ direction. The electronic localization near 2000 cm^{-1} is consistent with transport results, where the temperature-dependent resistivity of the $m = 2$ compound shows nonmetallic behavior with an activation energy about 0.084 eV (∼700 cm^{-1}) along c.[24] Judging from the energy and polarization of the 2000 cm^{-1} feature, this localization may originate from the

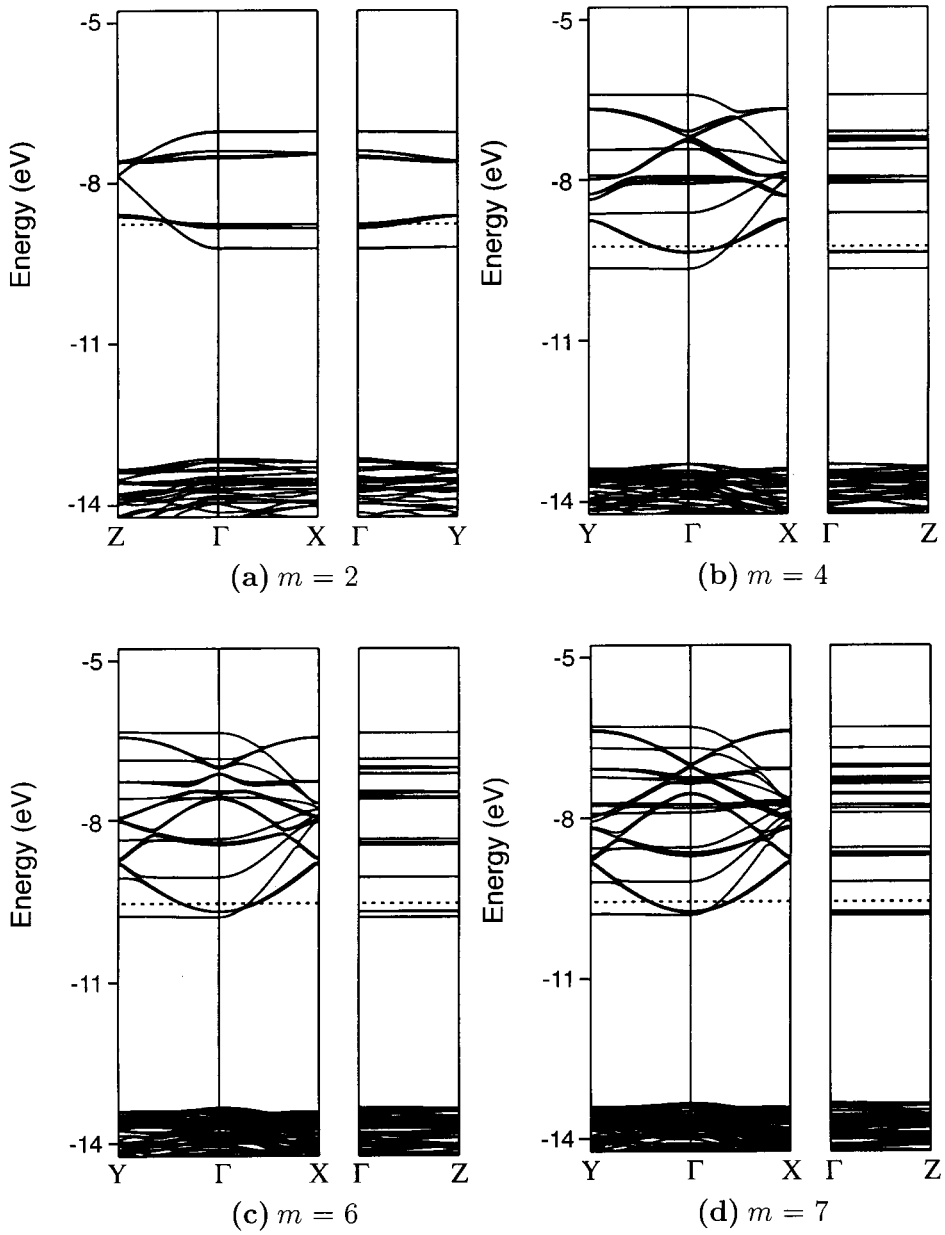

Figure 4. Dispersion relations of the top portion of the *p*-block bands and the t_{2g}-block bands calculated for the $m = 2$, 4, 6, and 7 MPTBs. $\Gamma = (0, 0)$, $X = (\pi/a, 0)$, $Y = (\pi/b, 0)$, $Z = (0, 2\pi/c)$.

two quarter-filled narrow bands along the *c* direction.[18] Similar localization phenomena are also observed in the other weak metals, such as organic conductors.[38,39]

The low-frequency *ab*-plane response of the $m = 4$ material is dominated by a giant bound-carrier absorption with a sharp edge near 500 cm^{-1} (Figures 3 and 7). The center frequency of the feature is nearly the same along both the *a* and *b* directions. Note that considerable residual optical conductivity remains in the low-frequency range despite the strong gap-like absorption, suggesting that the gap might not be fully open. Although the dc conductivity is in reasonable agreement with the value estimated from the low-frequency spectra, the strong low-energy charge localization is unexpected because the transport results indicate that the $m = 4$ compound displays a metallic response.[25] It is possible that the free-carrier (Drude) response appears well below 50 cm^{-1}, which is out of the range of our investigation, similar to the case of $(TMTSF)_2PF_6$.[40] This infrared bound-carrier absorption is relatively temperature-independent,[41] reminiscent of the large polaron response.[42]

The *ab*-plane spectra of the $m = 7$ compound display a rising low-frequency conductivity, consistent with the expected metallic response at 300 K (Figures 3 and 7). The dc conductivity estimated from extrapolation of σ_1-

(38) Jones, B. R.; Olejniczak, I.; Dong, J.; Pigos, J. M.; Zhu, Z.-T.; Garlach, A. D.; Musfeldt, J. L.; Koo, H.-J.; Whangbo, M.-H.; Schlueter, J. A.; Ward, B. H.; Morales, E.; Kini, A. M.; Winter, R. W.; Mohtasham, J.; Gard, G. L. *Chem. Mater.* **2000**, *12*, 2490.

(39) Pigos, J. M.; Jones, B. R.; Zhu, Z.-T.; Musfeldt, J. L.; Homes, C. C.; Koo, H.-J.; Whangbo, M.-H.; Schlueter, J. A.; Ward, B. H.; Wang, H. H.; Geiser, U.; Mohtasham, J.; Winter, R. W.; Gard, G. L. *Chem. Mater.* **2001**, *13*, 1326.

(40) Vescoli, V.; Degiorgi, L.; Dressel, M.; Schwartz, A.; Henderson, W.; Alavi, B.; Grüner, G.; Brinckmann, J.; Virosztek, A. *Phys. Rev. B* **1999**, *60*, 8019.

(41) Zhu, Z.-T. Ph.D. Dissertation, State University of New York at Binghamton, Binghamton, NY, 2001.

(42) Emin, D. *Phys. Rev. B* **1993**, *48*, 13691.

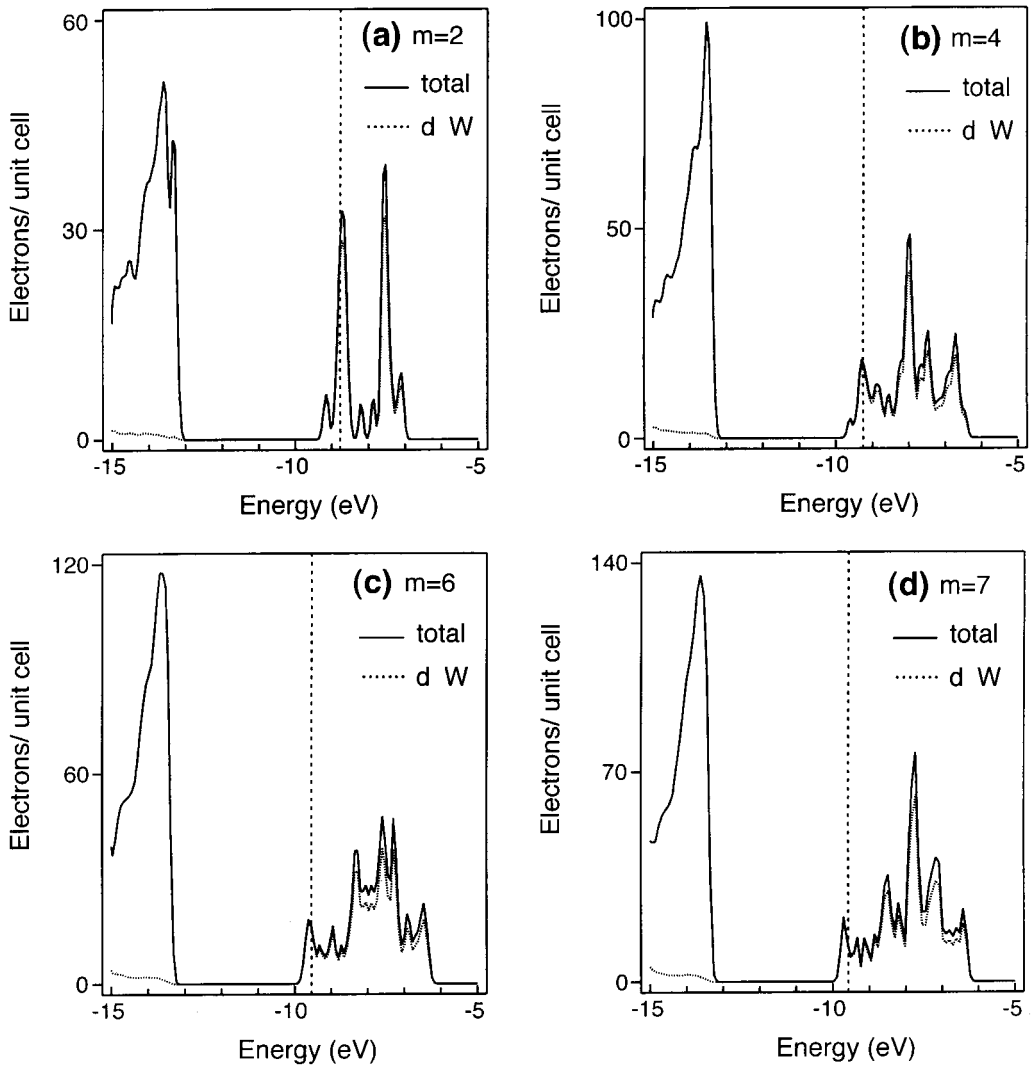

Figure 5. Density of states (DOS) of the top portion of the *p*-block bands and the t_{2g}-block bands calculated for the $m = 2$, 4, 6, and 7 MPTBs. Solid line, total DOS; dashed line, partial DOS due to tungsten d levels.

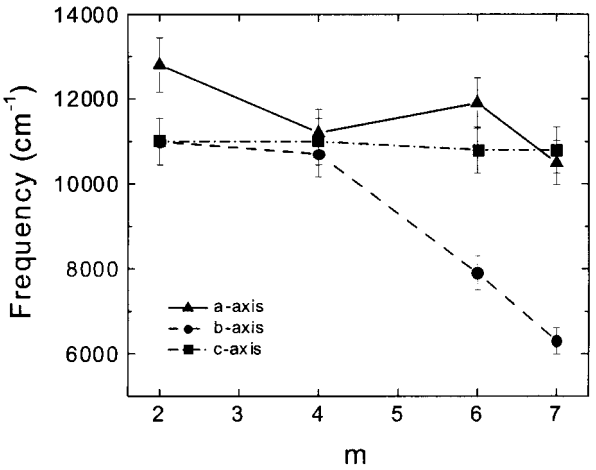

Figure 6. Center frequencies of the intra-t_{2g} d → d excitation as a function of *m* along the three principal-axis directions of $(PO_2)(WO_3)_{2m}$. The lines guide the eye.

(ω) to zero frequency is, however, somewhat higher than that obtained from transport measurements. In addition to the rising low-frequency conductivity that is characteristic of a metallic response, the *ab*-plane spectra of the $m = 7$ material display extra oscillator strength in the middle-infrared region. This observation, combined with the clear electronic localization in the $m = 2$ and 4 compounds, suggests a hidden bound-carrier contribution in the spectra of the $m = 7$ MPTB. To test this hypothesis, a Drude−Lorentz model was employed to fit $\sigma_1(\omega)$ along the *b* direction (inset of the lower right-hand panel, Figure 7). Here, a Drude component accounts for the free-carrier response, and a Lorentz oscillator accounts for the bound-carrier contribution. The fit results indicate that the $m = 7$ material should not be considered as a simple metal, even at 300 K, because of the presence of a bound-carrier localization along *b*.[43] In fact, this *b*-polarized charge localization becomes quite pronounced at low temperatures, stealing oscillator strength from the free-carrier part and dominating the infrared response.[33] Recall that the band structure along *b* (Figure 4) displays both flat and dispersive bands, making this direction most susceptible to localization effects.

The spectral results on this series of MPTBs show that an unusual bound-carrier absorption in the infra-

(43) The far-infrared response of the $m = 6$ material is unavailable, as mentioned previously in the Experimental Section. We suspect that a pseudogap structure is present in $m = 6$ as well, although missing far-infrared data precludes a detailed analysis.

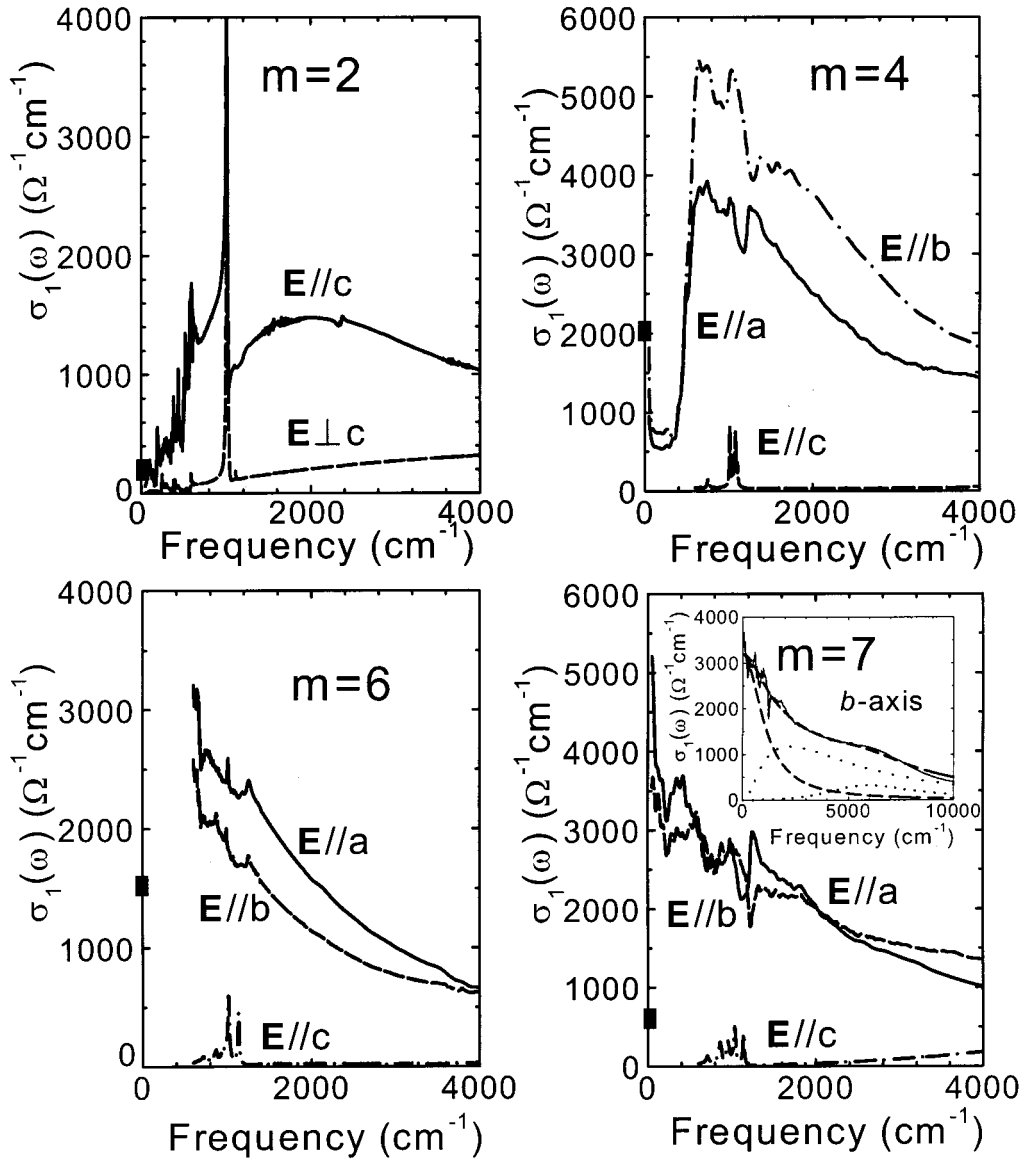

Figure 7. Close-up view of the optical conductivities of the $m = 2$, 4, 6, and 7 MPTB compounds at 300 K. The dc conductivity of each material[23−25,29] is indicated by a solid square at zero frequency. The inset in the lower right-hand panel shows the Drude−Lorentz fit for the *b*-axis spectrum of the $m = 7$ compound.

red region seems to be a ubiquitous feature of the tungsten bronze electrodynamics. The persistence of the psuedogap above the density wave transitions (and even up to room temperature) might be a manifestation of fluctuation effects in these 2D materials.[44] It is especially interesting that the superconducting ground state is ultimately stabilized in the $m = 7$ material despite this charge localization.[45]

2. Interlayer Response. The low-frequency electronic response along the interlayer direction is of recent interest in a number of Q2D materials, such as cuprates and organic superconductors.[46,47] This is because the interlayer interaction may play an important role in stabilizing superconductivity in these materials. The $m = 4$, 6, and 7 tungsten bronze optical conductivities are very similar along the interlayer direction, with modest electronic backgrounds and strong phonon features. This result is consistent with a nonmetallic, possibly incoherent, transport picture, similar to the optical response of underdoped cuprates[46] and organic superconductors[47] along the interlayer direction.

D. *m*-Dependent Interlayer Phonons. A large number of infrared-active phonon modes are expected in MPTBs because of their complicated unit cells and low site symmetry, according to a group theory analysis.[32] For instance, 134 normal modes are anticipated for the $m = 4$ material. As shown in Figure 3, the vibrational features are strong along the *c* axis, whereas the phonons are heavily screened (but not completely absent) in the conducting *ab* plane, confirming the Q2D character of the MPTBs.[48] Figure 8 displays the interlayer *c*-axis vibrational features for $m = 4$, 6, and 7

(44) Fluctuation effects are well-known to be important in 1D CDW materials. (For reference, see: Grüner, G. *Density Waves in Solids*; Addison-Wesley: New York, 1994.)

(45) A detailed discussion of the low-temperature optical behavior of the $m = 7$ compound is presented elsewhere.[33]

(46) Basov, D. N.; Woods, S. I.; Katz, A. S.; Singley, E. J.; Dynes, R. C.; Xu, M.; Hinks, D. G.; Homes, C. C.; Strongin, M. *Science* **1999**, *283*, 49.

(47) McGuire, J. J.; Rõom, T.; Pronin, A.; Timusk, T.; Schlueter, J. A.; Kelly, M. E.; Kini, A. M. *Phys. Rev. B* **2001**, *64*, 094503.

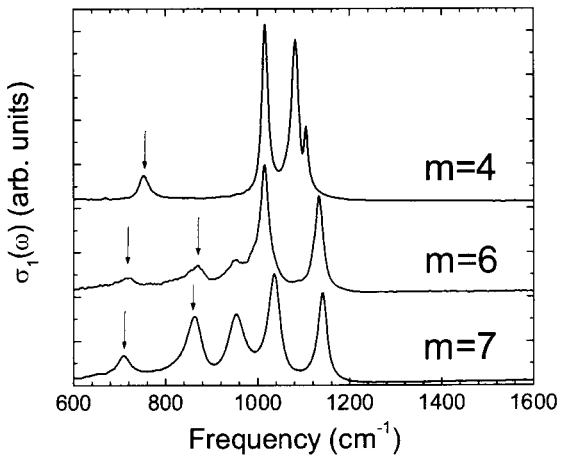

Figure 8. 300 K vibrational features along the *c*-axis polarization for the $m = 4$, 6, and 7 compounds. The spectra are offset for clarity. The arrows indicate the W−O stretching-related modes.

Table 2. Assignment of the *c*-Axis Vibrational Features for $m = 4$, 6, and 7 MPTBs

compound	frequency (cm^{-1})	assignment
$m = 4$	1106, 1081, 1016	ν_3, P−O asymmetric stretching
	–	ν_1, P−O symmetric stretching
	754	W−O stretching
$m = 6$	1133,1015	ν_3, P−O asymmetric stretching
	951	ν_1, P−O symmetric stretching
	863, 717	W−O stretching
$m = 7$	1140,1035	ν_3, P−O asymmetric stretching
	955	ν_1, P−O symmetric stretching
	860, 710	W−O stretching

samples.[49] Vibrational mode assignments are listed in Table 2. In the investigated frequency range, phonons are observed between 600 and 1400 cm^{-1}. A single W−O stretching mode at 754 cm^{-1} is seen in the *c*-axis spectrum of the $m = 4$ compound. The red shift of this feature with *m* (717 cm^{-1} for $m = 6$ and 710 cm^{-1} for $m = 7$) is in line with a more relaxed lattice and less distorted WO_6 octahedra with increasing *m*. The feature observed near 860 cm^{-1} in the *c*-axis spectra of the $m = 6$ and 7 materials is also a W−O stretching mode. The intensity of this mode grows with increasing *m*, becoming the dominant W−O stretching vibration in the $m = 7$ material. Several W−O-related bending modes certainly appear in the frequency range below 600 cm^{-1}.

The strongest vibrational modes in Figure 8 are related to P−O stretching motion. In an ideal PO_4 tetrahedron with T_d symmetry, ν_3 (∼1080 cm^{-1}) and ν_4 (∼500 cm^{-1}) are both infrared- and Raman-active; ν_1 (∼970 cm^{-1}) and ν_2 (∼385 cm^{-1}) are only Raman-active.[50] The site symmetry of the $m = 4$, 6, and 7 compounds is C_1 according to the crystal space group. Therefore, all nine PO_4 tetrahedral modes are infrared-active: ν_3 and ν_4 split into triplets, ν_2 splits into a doublet, and ν_1 is activated.[50] As shown in Table 2, ν_1 is strongly infrared-active in the spectra of $m = 6$ and 7, and ν_3 does appear as a doublet. In the spectrum of the $m = 4$ sample, ν_3 is a triplet, consistent with C_1 site symmetry. Therefore, we conclude that the PO_4 tetrahedra are also less distorted with increasing *m*. In infrared transmission studies on the $m = 6$ compound, we observed a new low-temperature mode at 1099 cm^{-1},[32] suggesting that ν_3 changes from a doublet to a triplet along the interlayer direction with decreasing temperature.

IV. Conclusion

We report the 300 K polarized reflectance spectra and calculated electronic band structures of a series monophosphate tungsten bronzes, $(PO_2)_4(WO_3)_{2m}$ ($m = 2$, 4, 6, 7). These materials have several layers of corner-sharing WO_6 octahedra separated by one PO_4 layer, leading to an octahedral layer thickness that is "tunable" with *m*. In the optical regime, the spectra of the $m = 2$, 4, 6, and 7 materials display an anisotropic electronic excitation originating from the W intra-t_{2g} d → d transition. The intensity and frequency of the intra-t_{2g} d → d excitation vary with the octahedral layer thickness. Several vibrational modes along the interlayer direction of the $m = 4$, 6, and 7 compounds also change with *m*. These results are consistent with the lattice becoming softer with increasing *m*. The low-frequency electrodynamics of the monophosphate tungsten bronzes shows a gap or pseudogap feature in the infrared region, demonstrating a ubiquitous bound-carrier response in these tungsten bronzes.

Acknowledgment. Work performed at SUNY-Binghamton, the University of Tennessee, and North Carolina State University was supported by the Materials Science Division, Office of Basic Energy Sciences, at the U.S. Department of Energy under Grants DE-FG0201-ER45885 (UT) and DE-FG02-86ER45259 (NCSU). Work performed at Rutgers University was supported by the Division of Materials Research at the National Science Foundation under Grant DMR-9907963.

CM011675J

(48) A detailed discussion of the *ab*-plane phonons in the $m = 7$ can be found in ref 33.

(49) The interlayer response of the $m = 2$ material is not available because of the needlelike crystal shape.

(50) Ross, S. D. *Inorganic Infrared and Raman Spectra*; McGraw-Hill: London, 1972.